ELSEVIER

www.elsevier.com/locate/ica
Inorganica Chimica Acta 320 (2001) 159–166

Inorganica Chimica Acta

Syntheses, structures and magnetic properties of mono- and di-manganese inclusion compounds

Changneng Chen [a], Hongping Zhu [a], Deguang Huang [a], Tingbin Wen [a], Qiutian Liu [a,*], Daizheng Liao [b], Jianzhong Cui [b]

[a] *State Key Laboratory of Structural Chemistry, Fujian Institute of Research on the Structure of Matter, Chinese Academy of Sciences, Fuzhou, Fujian 350002, China*

[b] *Department of Chemistry, Nankai University, Tianjin 300071, China*

Received 24 January 2001; accepted 17 May 2001

Abstract

Mono- and di-manganese inclusion compounds **1** and **2** are reported. Two mono-manganese molecules $Mn(bpy)_2(NO_3)_2$ (bpy = 2,2′-bipyridine) and $[Mn(bpy)_2(NO_3)(H_2O)]\cdot NO_3$ coexist in the mole ratio of 1:1 in the structure of **1**, while two di-manganese molecules $[Mn_2O(bpy)_2(phtha)_2(H_2O)_2]\cdot(NO_3)_2$ (phtha = phthalate) and $[Mn_2O(bpy)_2(phtha)_2(NO_3)(H_2O)]\cdot NO_3$ in the structure of **2**. Refluxing $Mn(NO_3)_2$/bpy/phthalic acid reaction mixtures in CH_3CN leads to the isolation of **1**, further concentration of the reaction solution in raising temperature results in **2**. The Mn_1 and Mn_2 units in the inclusion compounds **1** and **2** are similar to other reported Mn_1 and Mn_2 analogs, respectively. The Jahn–Teller distortion was observed to give rise to the elongation along the $O_{terminal}$–Mn–$O_{carboxyl}$ axes for all the four Mn(III) sites in **2**, leading to unexpected longer Mn(III)–O_{aqua} than Mn(II)–O_{aqua} in **1**. Extensive hydrogen bonding interactions among H_2O, NO_3^- and COOH were observed in the two inclusion compounds. Cyclic voltammetry of **2** in DMF displays two quasi-reversible redox couples at $+0.10/+0.22$ and $-0.43/-0.36$ V assigned to the Mn(III)Mn(IV)/2Mn(III) and 2Mn(III)/Mn(III)Mn(II), respectively. Variable temperature magnetic susceptibilities of **1** and **2** were measured. The data were fit to a model including axial zero-field splitting term and a good fit was found with $D = 1.77\ cm^{-1}$, $g = 1.98$ and $F = 1.48 \times 10^{-5}$ for **1**. For **2**, the least-squares fitting of the experimental data led to $J = 2.37\ cm^{-1}$, $g = 2.02$ and $D = 0.75\ cm^{-1}$ with $R = 1.45 \times 10^{-3}$. © 2001 Elsevier Science B.V. All rights reserved.

Keywords: Crystal structures; Magnetic properties; Manganese complexes; Phthalate complexes; Inclusion complexes

1. Introduction

During the past two decades, modeling the structure, the spectroscopic properties and the reactivity of manganese cluster in photosystem II are of major interest to inorganic chemists. A great deal of Mn complexes with Mn(II, III, IV) centers and O,N-donor atoms have been synthesized as a model of the water oxidation center [1]. Di-manganese complexes with μ-oxo-bis-μ-carboxylato unit have attracted more attention since the unit was proposed as the active site in the ribonucleotide reductase [2]. In the previous known researches, the use of bidentate and tridentate N-containing ligands such as bipyridine and carboxylic acid gives rise to the di-manganese complexes containing the μ-oxo-bis-μ-carboxylato unit [3,4]. Up to now acetate and benzoate have always been reported as the bis-μ-carboxylato unit, while the use of dicarboxylic acid in the reaction has rarely been studied for preparing poly-manganese compound [5]. We are interested in the formation of the di-manganese complexes in the presence of dicarboxylic acid, since this assembly may have potential interest for the further aggregate of the manganese cluster, leading to a polynuclear Mn cluster. Here we report the syntheses of mono- and di-manganese complexes and their structural characterization. Their magnetic properties are also discussed.

* Corresponding author. Fax: +86-591-371-4946.
E-mail address: lqt@ms.fjirsm.ac.cn (Q. Liu).

0020-1693/01/$ - see front matter © 2001 Elsevier Science B.V. All rights reserved.
PII: S0020-1693(01)00489-3

2. Experimental

All manipulations were performed under aerobic conditions with materials as received.

2.1. Synthesis

2.1.1. $[Mn_2(bpy)_4(NO_3)_3(H_2O)]NO_3$ (1) and $[Mn_4(bpy)_4(o\text{-}HOOCC_6H_4COO)_4(\mu\text{-}O)_2(H_2O)_3(NO_3)](NO_3)_3$ (2)

Solid 2,2′-bipyridine (0.50 g, 3.20 mmol), $Mn(NO)_3{\cdot}4H_2O$ (0.64 g, 2.55 mmol), and phthalic acid (0.41 g, 2.47 mmol) were mixed in 50 ml of acetonitrile and stirred for 3 h at room temperature (r.t.). Then the solution was continuously stirred and refluxed for 2 h. After filtration to remove the light yellow precipitate, the filtrate was allowed to stand for several days to deposit bright yellow crystals which were collected and dried in vacuo, yielding 0.45 g (yield 56% based on bpy) of **1**. *Anal*. Found: C, 48.19; H, 3.39; Mn, 10.61; N, 16.89. Calc. for $C_{40}H_{34}Mn_2N_{12}O_{13}$: C, 48.01; H, 3.42; Mn, 10.98; N, 16.80%. IR (KBr, cm^{-1}): 3441 (m, br), 1594 (s), 1472 (m), 1437 (s), 1384(s), 1313 (w), 1247 (w), 1173 (w), 1150 (w), 1097 (w), 1058 (w), 1013 (m), 820 (w), 773 (s), 737 (m), 651 (w), 625 (w).

In the preceding procedure, the filtrate of reaction mixture containing **1** was concentrated at rising temperature to remove 30 ml of the solvent, accompanying the color change from light yellow to dark brown. The concentrated solution was allowed to stand at r.t. for several days to deposit dark brown crystals, which were collected and dried in vacuo, affording **2** with 14.5% yield based on phthalic acid. *Anal*. Found: C, 47.59; H, 3.17; Mn, 11.16; N, 9.39. Calc. for $C_{72}H_{58}Mn_4N_{12}O_{33}$: C, 47.02; H, 3.18; Mn, 11.95; N, 9.14%. IR (KBr, cm^{-1}): 3400 (m, br), 3112 (w), 1737 (s), 1610 (s), 1589 (m), 1447 (m), 1384 (s), 1307 (m), 1249 (w), 1173 (w), 1075 (w), 1034 (w), 826 (w), 771 (m), 728 (m), 652 (w), 477 (w), 334 (w).

Table 1
Crystallographic data for compounds **1** and **2**

Empirical formula	$C_{40}H_{34}Mn_2N_{12}O_{13}$	$C_{72}H_{68}Mn_4N_{12}O_{38}$
Formula weight	1000.67	1929.14
Temperature (°C)	20	20
λ(Mo Kα)	0.71069	0.71073
Space group	*Pbca* (no. 61)	*P*1 (no. 1)
Unit cell dimensions		
a (Å)	14.39(1)	10.007(2)
b (Å)	17.12(1)	10.284(2)
c (Å)	34.70(1)	20.283(4)
α (°)		78.98(3)
β (°)		80.95(3)
γ (°)		85.67(3)
V (Å^3)	8545(18)	2021.1(7)
Z	8	1
ρ_{calc} (g cm^{-3})	1.56	1.585
μ (mm^{-1})	0.64	0.713
R [a]	0.0585	0.0543
R_w [b]	0.0751	0.1407

1, $w = 1/[S^2(F) + (0.030F)^2 + 1.0] - F$; **2**, $w = 1/[S^2(F_o^2) + (0.1000P)^2 + 0.0000P]$, where $P = (F_o^2 + 2F_c^2)/3$.

[a] $R = \Sigma||F_o| - |F_c||/\Sigma|F_o|$.

[b] $R_w = [\Sigma w(|F_o| - |F_c|)^2/\Sigma wF_o^2]^{1/2}$.

2.2. X-ray crystallography and structure solution

Crystalline samples were selected from the reaction solutions for **1** and **2**, and were coated with epoxy resin and mounted. Data were collected on AFC 5R Rigaku diffractometer and Siemens Smart CCD for **1** and **2**, respectively. The data collections were performed using ω–2θ scan mode with the maximum θ of 26° for **1**, and ω mode in the range of $2.02 < \theta < 25.03°$ for **2**. For **1** 9232 unique reflections were obtained for which Lorentz polarization correction was applied. For **2** 8594 unique reflections obtained were reduced by Siemens Saint and corrected by SADABS (0.7594–1.0000). The crystallographic data of the two compounds are listed in Table 1.

The structure was solved by a combination of direct methods and Fourier techniques for each compound and the Mn atoms were located from initial E-maps. The positions of the remaining non-hydrogen atoms were obtained from subsequent iterations of least-squares refinement and difference Fourier maps phased on the already located atoms. Hydrogen atoms were geometrically located and added to the structure factor calculations but their positions were not refined. Compound **2** contains both almost the same dinuclear manganese cluster units in cell which seems to have $P\bar{1}$ feature. However, the refinement with a symmetrical center leaded to a vague description of a tetranuclear Mn cluster. Consequently, space group *P*1 was selected and used to give two Mn_2 clusters coexisting in an inclusion compound. The structures of **1** and **2** were refined by full-matrix least-squares technique using anisotropic thermal parameters for all the non-hydrogen atoms except for the oxygen atom (O45) in the solvate H_2O of **2**. One of the oxygen atoms in external NO_3^- group which is not coordinated to the Mn atom in **2** was found to be disordered at two positions (O31 and O31′) with the occupancies of 0.2 and 0.8, respectively. For **1** the final refinement included 604 variable parameters for 3089 [$I > 1.0\sigma(I)$] reflections, and converged to $R = 0.0585$ and $R_w = 0.0751$. For **2**, 1139 variable parameters and 6041 [$I > 2.0\sigma(I)$] reflections, of which one reflection (*hkl* 0, 0, 1) with too high $\Delta(F^2)$/esd value was omitted, were refined to give final $R = 0.0543$ and $R_w = 0.1407$. The highest and the minimum residual peaks in the final difference Fourier map had a height of 0.37 and -0.09 e Å^{-3} for **1**, and 0.638 and -0.513 e Å^{-3} for **2**. All calculations were per-

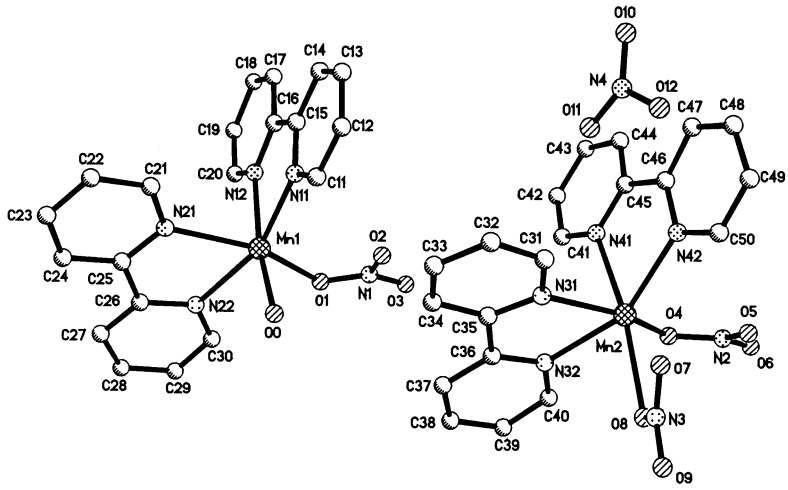

Fig. 1. ORTEP representation of the two components in compound **1** at the 30% probability level.

formed by using MULTAN-83 (MolEN) program [6] for **1** and SHELXTL-93 [7] for **2**.

2.3. Other physical measurements

The IR spectra were recorded on a Bio-Rad FTS-40 Model spectrophotometer. The variable temperature susceptibilities were measured on a Model CF-1 superconducting extraction sample magnetometer with the crystalline sample kept in a capsule at 5–300 K. Diamagnetic corrections of -509×10^{-6} and -466.5×10^{-6} emu mol^{-1} were used for compounds **1** and **2**, respectively. Electrochemical measurement was performed in the cyclic voltammetric mode on a CV-1B cyclic voltammeter in DMF with an SCE reference electrode, graphite working electrode, and Pt auxiliary electrode. The supporting electrolyte was Et_4NBF_4.

3. Results and discussion

3.1. Synthesis

Some mononuclear Mn complexes [8] with bpy ligand have been synthesized by reaction of bpy with simple inorganic Mn salt and have been structurally characterized. Compound **1** is an inclusion compound containing $[Mn(bpy)_2(NO_3)(H_2O)]NO_3$ and $Mn(bpy)_2(NO_3)_2$ molecules in a molar ratio of 1:1. Though the former has been reported [8a], compound **1** is still an interesting example among the mononuclear Mn complexes for structural and chemical studies. Especially, the further reaction of **1** with phthalic acid in the reaction solution caused condensation of the mononuclear complex and produced di-manganese compound **2**. It is interesting that **2** is also an inclusion compound composed of two di-manganese molecules $[Mn_2(\mu\text{-}O)(bpy)_2(o\text{-}HOOCC_6H_4COO)_2(H_2O)_2](NO_3)_2$ and $[Mn_2(\mu\text{ - }O)(bpy)_2(o\text{ - }HOOCC_6H_4COO)_2(H_2O)(NO_3)](NO_3)$ in a molar ratio of 1:1. Recently, linking simple Mn species by poly-functional ligands to produce higher nuclearity of manganese complex has attracted more attention [9,10]. Compound **1** can be seen as a building block to construct the di-manganese aggregate **2**. It is noted that the two mono-manganese components wrapped up in **1** are available to aggregate with each other to produce the di-manganese aggregate with terminal ligands H_2O or NO_3^-. On heating and concentrating the reaction solution, a peripheral basic bpy ligand would be abstracted by phthalic acid from **1** to give an intermediate fragment, which was oxidized by air and linked together to give the di-Mn(III) species. Similar di-Mn(III) complexes have been reported, which were formed in an assembly system in the presence of an oxidizer, such as MnO_4^- [3b]. A condensation mechanism has been suggested by Rajasekharan [3c] to explain the formation of $[Mn_2(\mu\text{-}O)(bpy)_2(OAc)_2(H_2O)(NO_3)](ClO_4)$, in which μ-O comes from the dehydration of hydroxyl groups contained in the Mn–OH moieties. It may be reasonable to consider that the bridging μ-oxo anion results from the dehydration of the Mn(III)–OH group, which comes from the oxidation of the Mn(II) site and then the deprotonation of the aqua ligating to the oxidized Mn site.

3.2. Structure

The structure of the inclusion compound **1** is represented in Fig. 1. Selected bond distances and angles are listed in Table 2. The structure consists of two mononuclear Mn molecules $Mn(bpy)_2(NO_3)_2$ and $[Mn(bpy)_2(NO_3)(H_2O)]NO_3$. The structure of the latter has been reported by Chen [8a], and the structure of the former is also normal for the mononuclear Mn complexes containing the $[Mn(bpy)_2]^{2+}$ core. The ligands form

a distorted octahedral coordination sphere about the Mn atom with the bpy bite angle N–Mn–N ranging from 71.1 to 72.4° and the Mn–N distance ranging from 2.248 to 2.366 Å. These values are close to those found in other mononuclear Mn(II) bpy complexes [8]. It is noted that in the inclusion compound the Mn–N bond lengths *trans* to $O_{nitrate}$, N_{bpy} and O_{aqua} average 2.316(30), 2.269(10) and 2.250(6) Å, respectively, showing stronger *trans*-effect of the NO_3^- group than the other two. A larger O–Mn–O angle (98.4°) is found in $[Mn(bpy)_2(NO_3)(H_2O)]NO_3$ than that in $Mn(bpy)_2(NO_3)_2$ (87.0°). This seems to be in contradiction with the larger stereo effect of NO_3^- than that of H_2O. However, strong hydrogen bonding interactions between ligated H_2O and discrete NO_3^- (O0···O10, 2.59 Å), and between the aqua and ligated NO_3^- belonging to the other molecule (O0···O5, 2.76 Å) were observed as shown in Fig. 2. These interactions enable the O_{aqua}–Mn–$O_{nitrate}$ angle in $[Mn(bpy)_2(NO_3)(H_2O)]^+$ to become larger.

Table 2
Selected bond lengths (Å) and bond angles (°) for compound **1**

Mn1–O0	2.133(6)	Mn2–O4	2.236(6)
Mn1–O1	2.275(6)	Mn2–O8	2.359(8)
Mn1–N11	2.248(6)	Mn2–N31	2.262(6)
Mn1–N12	2.250(6)	Mn2–N32	2.286(7)
Mn1–N21	2.319(6)	Mn2–N41	2.366(7)
Mn1–N22	2.289(6)	Mn2–N42	2.254(6)
O0–Mn1–O1	98.4(2)	O4–Mn2–O8	87.0(2)
O0–Mn1–N11	94.8(2)	O4–Mn2–N31	154.8(2)
O0–Mn1–N12	167.1(2)	O4–Mn2–N32	86.4(2)
O0–Mn1–N21	92.3(2)	O4–Mn2–N41	80.1(3)
O0–Mn1–N22	92.4(2)	O4–Mn2–N42	102.7(2)
O1–Mn1–N11	114.1(2)	O8–Mn2–N31	98.7(3)
O1–Mn1–N12	86.2(2)	O8–Mn2–N32	77.4(3)
O1–Mn1–N21	153.3(2)	O8–Mn2–N41	160.9(2)
O1–Mn1–N22	83.9(2)	O8–Mn2–N42	125.8(3)
N11–Mn1–N12	72.4(2)	N31–Mn2–N32	71.1(2)
N21–Mn1–N22	71.2(2)	N41–Mn2–N42	71.2(2)
N11–Mn1–N22	159.3(2)	N32–Mn2–N42	155.0(2)
N12–Mn1–N21	88.7(2)	N32–Mn2–N41	87.8(2)
N11–Mn1–N21	89.1(2)	N31–Mn2–N41	87.6(2)
N12–Mn1–N22	100.1(2)	N31–Mn2–N42	93.9(2)

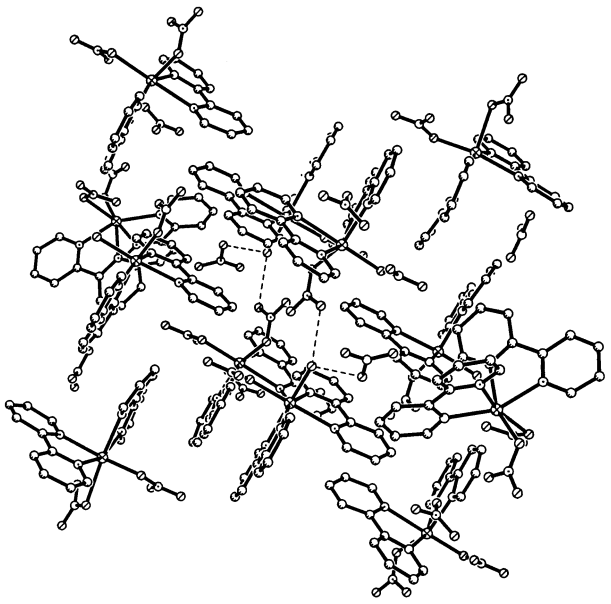

Fig. 2. Packing diagram of unit cell of **1**. Hydrogen bonds are indicated by dotted lines. The peripheral hydrogen bonds have been omitted.

Fig. 3 illustrates the structure of the other inclusion compound **2**. It consists of two di-manganese cluster cations, $[Mn_2(\mu\text{-}O)(bpy)_2(phtha)_2(H_2O)_2]^{2+}$ and $[Mn_2(\mu\text{-}O)(bpy)_2(phtha)_2(H_2O)(NO_3)]^+$, three nitrate anions as well as five solvate H_2O molecules. Selected bond distances and angles are listed in Table 3. It is necessary to point out that the structural difference of the two components constructing the inclusion compound is displayed only in their terminal ligands. A series of di-manganese compounds have been reported some of which were suspected to be a mixture [3b,c] of two Mn_2 clusters (H_2O, NO_3^- or OH^- ligation) with indefinite proportion. This implies that the terminal ligands in these compounds are labile and easy to exchange with each other, leading to the formation of the mixture that is difficult to purify, or in the rare situation, leading to the formation of di-molecule inclusion compounds, such as **1** and **2**. Both di-manganese ions in **2** possess similar structural parameters as shown in Table 3, except for the identity of the terminal ligands (NO_3^- and H_2O). In fact, all the atoms of the two Mn_2 components are related by a symmetrical center located in the middle of the line joining two Mn(III) sites (Mn2···Mn4 and Mn1···Mn3), except the atoms in the terminal ligands. In comparison to the other μ-oxo bis-μ-carboxylato di-manganese compounds, our di-manganese complexes exhibit a close similarity in the structural parameters of the core $Mn(III)_2(\mu\text{-}O)(\mu\text{-}RCOO)_2$, such as Mn···Mn, Mn–$O_{oxo}$, Mn–$O_{aqua}$, Mn–$O_{carboxyl}$, and Mn–O–Mn values (Table 4), exhibiting that the terminal ligands (NO_3^-, H_2O, Cl^-, or N_3^-) ligating to the Mn site have no serious effect on their core structures. The evidence for a Jahn–Teller elongation of Mn(III) with high spin d^4 was observed. The Mn–$O_{carboxyl}$ distances are divided into two sets differing by 0.17–0.2 Å, and the Mn–O_{aqua} distances (2.182, 2.191, 2.256 Å) for the Mn^{3+} oxidation state are unexpectedly longer than that (2.133 Å) in **1** and other Mn(II) complexes [8a,c]. It is reasonable to consider that the Jahn–Teller distortion gives rise to the elongation along the $O_{terminal}$–Mn–$O_{carboxyl}$ axes for all the Mn(III) sites in **2**. Interestingly, in compound **2** the longest Mn–O_{aqua} distance is Mn2–O24 of 2.256 Å, this even longer distance is probably due to the hydrogen bonding (O22···O24, 2.865 Å) with the NO_3^- group coordinated

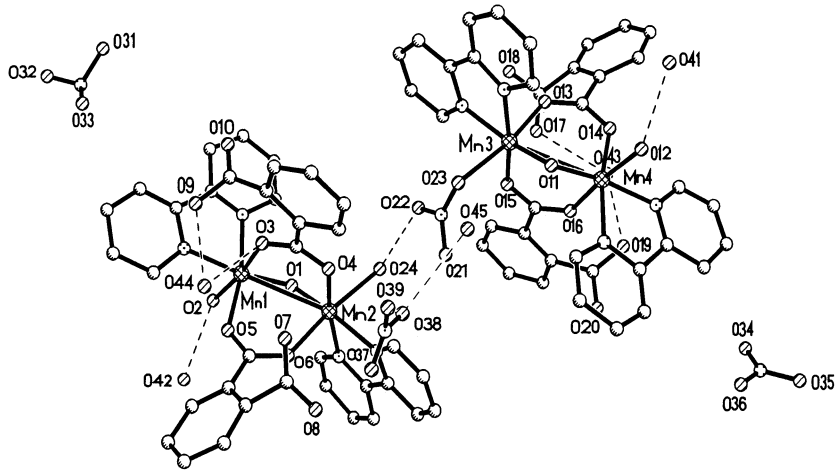

Fig. 3. Structure of compound **2** showing two Mn_2 units, anions and solvate H_2O molecules. Hydrogen bonding interactions between the components are also shown by dotted lines.

Table 3
Selected bond lengths (Å) and bond angles (°) for compound **2**

$[Mn_2O(\mu\text{-phth})_2(bpy)_2(H_2O)_2]^{2+}$				$[Mn_2O(\mu\text{-phth})_2(bpy)_2(H_2O)(NO_3)]^{+}$			
Mn1–Mn2	3.148(3)			Mn3–Mn4	3.155(3)		
Mn1–O1	1.769(9)	Mn2–O1	1.776(11)	Mn3–O11	1.773(10)	Mn4–O11	1.839(10)
Mn1–O5	1.999(10)	Mn2–O4	2.003(10)	Mn3–O15	1.938(11)	Mn4–O14	1.927(11)
Mn1–N1	2.046(13)	Mn2–N3	2.087(12)	Mn3–N6	2.040(13)	Mn4–N8	2.049(13)
Mn1–N2	2.070(12)	Mn2–N4	2.105(13)	Mn3–N5	2.047(12)	Mn4–N7	2.087(13)
Mn1–O3	2.171(11)	Mn2–O6	2.172(11)	Mn3–O13	2.125(10)	Mn4–O16	2.135(11)
Mn1–O2	2.182(11)	Mn2–O24	2.256(12)	Mn3–O23	2.311(10)	Mn4–O12	2.191(11)
O1–Mn1–O5	98.4(5)	O1–Mn2–O4	97.5(4)	O11–Mn3–O15	99.3(5)	O11–Mn4–O14	100.9(5)
O1–Mn1–N1	93.5(5)	O1–Mn2–N3	91.4(5)	O11–Mn3–N6	167.5(5)	O11–Mn4–N8	170.3(5)
O5–Mn1–N1	168.1(5)	O4–Mn2–N3	170.8(5)	O15–Mn3–N6	93.1(5)	O14–Mn4–N8	88.8(5)
O1–Mn1–N2	170.4(5)	O1–Mn2–N4	168.2(5)	O11–Mn3–N5	89.2(5)	O11–Mn4–N7	91.4(5)
O5–Mn1–N2	90.6(5)	O4–Mn2–N4	94.2(5)	O15–Mn3–N5	171.4(5)	O14–Mn4–N7	167.5(5)
N1–Mn1–N2	77.6(5)	N3–Mn2–N4	76.9(5)	N6–Mn3–N5	78.3(5)	N8–Mn4–N7	78.9(5)
O1–Mn1–O3	91.4(4)	O1–Mn2–O6	96.8(4)	O11–Mn3–O13	99.2(5)	O11–Mn4–O16	91.7(4)
O5–Mn1–O3	91.3(5)	O4–Mn2–O6	89.5(4)	O15–Mn3–O13	87.3(5)	O14–Mn4–O16	90.2(5)
N1–Mn1–O3	89.1(5)	N3–Mn2–O6	92.1(4)	N6–Mn3–O13	82.4(5)	N8–Mn4–O16	87.5(5)
N2–Mn1–O3	85.1(4)	N4–Mn2–O6	84.3(4)	N5–Mn3–O13	91.7(5)	N7–Mn4–O16	87.3(5)
O1–Mn1–O2	96.8(5)	O1–Mn2–O24	94.7(5)	O11–Mn3–O23	92.2(4)	O11–Mn4–O12	93.0(4)
O5–Mn1–O2	87.1(4)	O4–Mn2–O24	84.2(4)	O15–Mn3–O23	89.0(4)	O14–Mn4–O12	91.0(5)
N1–Mn1–O2	90.8(5)	N3–Mn2–O24	92.6(4)	N6–Mn3–O23	86.8(4)	N8–Mn4–O12	87.5(5)
N2–Mn1–O2	87.0(5)	N4–Mn2–O24	85.5(5)	N5–Mn3–O23	90.3(4)	N7–Mn4–O12	90.5(5)
O3–Mn1–O2	171.9(4)	O6–Mn2–O24	167.5(5)	O13–Mn3–O23	168.4(4)	O16–Mn4–O12	174.8(5)
Mn1–O1–Mn2	125.2(6)			C71–O13–Mn3	126.6(10)	Mn3–O11–Mn4	121.8(5)
C51–O3–Mn1	130.4(9)	C51–O4–Mn2	125.4(9)	C81–O15–Mn3	130.4(10)	C71–O14–Mn4	128.5(10)
C61–O5–Mn1	131.8(10)	C61–O6–Mn2	131.0(11)	N9–O23–Mn3	121.9(8)	C81–O16–Mn4	132.4(10)
C5–N1–Mn1	116.9(11)	C11–N3–Mn2	125.7(11)	C35–N5–Mn3	117.6(11)	C41–N7–Mn4	124.4(10)
C1–N1–Mn1	123.9(11)	C15–N3–Mn2	116.0(10)	C31–N5–Mn3	122.5(11)	C45–N7–Mn4	115.3(9)
C6–N2–Mn1	115.8(10)	C16–N4–Mn2	115.9(11)	C40–N6–Mn3	125.5(9)	C50–N8–Mn4	126.9(11)
C10–N2–Mn1	122.7(11)	C20–N4–Mn2	123.4(11)	C36–N6–Mn3	116.7(10)	C46–N8–Mn4	116.7(11)

to Mn3. The presence of the nitrate and carboxyl groups and the presence of coordinate and solvate H_2O molecules make extensive hydrogen bonding interactions in the lattice of the inclusion compound as shown in Fig. 3. All the hydrogen bonding interactions are listed in Table 5. The importance of the hydrogen bonding interactions for the formation of the inclusion compounds can also not be ignored. These hydrogen bonds make the two components (Mn_2 or Mn_1) inseparably combine with each other to become an inclusion compound. For **1** O0···O5 links the two Mn_1 components, while O22···O24 links the two Mn_2 components in **2**. The hydrogen bonding interactions including O45 must be mentioned which occur between two

Table 4
Comparison of the structural data for complexes containing $Mn_2(\mu\text{-O})(bpy)_2$bis-(μ-carboxylato) moiety

Complex	Mn–Mn	Mn–N	Mn–O (oxo)	Mn–O (aqua)	Mn–O (carboxyl)	$Mn–O_{oxo}–Mn$	Ref.
$[Mn_2O(\mu\text{-phth})_2(bpy)_2(H_2O)_2]^{2+}$	3.148(3)	2.077	1.773	2.219	2.001 2.172	125.2(6)	[a]
$[Mn_2O(\mu\text{-phth})_2(bpy)_2(H_2O)(NO_3)]^{+}$	3.155(3)	2.056	1.806	2.191	1.933 2.130	121.8(2)	[a]
$Mn_2O(\mu\text{-PhCOO})_2(bpy)_2(OH)(NO_3)$	3.141(1)	2.073	1.777	2.15 [b]	1.971 2.158	124.12(11)	[3b]
$[Mn_2O(\mu\text{-AcO})_2(bpy)_2(H_2O)_2]^{+}$	3.152(2)	2.071	1.797	2.286	1.943 2.170	122.7(2)	[3a]
$[Mn_2O(\mu\text{-AcO})_2(bpy)_2(H_2O)_2]^{+}$	3.139	2.064	1.787	2.315	1.936	123.0	[3c]
$[Mn_2O(\mu\text{-AcO})_2(bpy)_2(H_2O)(NO_3)]^{+}$	3.137(2)	2.069	1.786	2.224	1.939 2.180	122.9	[3c]

[a] This work.
[b] Mn–OH.

$Mn_2\cdots Mn_2$ moieties. In addition, to link to the NO_3^- group (O45···O21, 2.863 Å; O45···O23, 2.874 Å) coordinated to the $Mn_2\cdots Mn_2$ moiety, O45 links to COOH in the adjacent $Mn_2\cdots Mn_2$ moiety (O45···O18A, 2.822 Å), leading to the formation of molecular polymeric chains. A projection of the crystal packing is shown in Fig. 4, exhibiting the network structure of hydrogen bonding interactions for compound **2**.

3.3. Electrochemistry

The electrochemical property of the inclusion compound **2** has been examined by cyclic voltammetry shown in Fig. 5. A quasi-reversible redox was observed at $+0.10/+0.22$ V with broadened features. The exchange equilibrium between monodentate ligands and the solvent may make broad features for cyclic voltammetry. In comparison with the behavior of the other $Mn_2(III)(\mu\text{-O})_{1-2}(RCOO)_{2-1}$ species, [3a,4,11] the redox of compound **2** occurs in more negative potential. However, on the oxidation side, the scan to $+2.0$ V has not found additional oxidation features. So the redox at $+0.10/+0.22$ V would be assigned to the $Mn(III)_2/Mn(III)Mn(IV)$ couple. Interestingly, compound **2** exhibits the other quasi-reversible redox at $-0.43/-0.36$ V, showing more abundant redox features. It is considered that the participation of the dicarboxylic acid varies the electrochemical behavior of the $Mn(III)_2$ unit by intra- and intermolecular hydrogen bonding interactions which stabilize the $Mn(III)_2$ unit so as to avoid damage in the reduction process. The redox at $-0.43/-0.36$ V could be tentatively assigned to the $Mn(III)Mn(II)/Mn(III)_2$ couple.

3.4. Magnetic properties

Compound **1** consists of two mononuclear Mn(II) molecules. The two Mn(II) ions belonging to the respective molecules keep themselves apart from each other by at least 7.49 Å. It is believed that the two Mn(II) ions do not undergo magnetic exchange interaction though the hydrogen bonding interactions were found between the two molecules. The magnetic properties of **1** are illustrated as the temperature dependence

Table 5
Hydrogen bonding interactions (Å) in inclusion compound **2**

O24···O22	2.865	Ligand to ligand $H_2O\cdots NO_3$
O24···O4	2.860	Ligand to ligand $H_2O\cdots COOH$
O45···O21	2.863	Solvent to ligand $H_2O\cdots NO_3$
O45···O23	2.874	Solvent to ligand $H_2O\cdots NO_3$
O44···O18A	2.822	Solvent to ligand $H_2O\cdots COOH$
O2···O42	2.689	Ligand to solvent $H_2O\cdots H_2O$
O12···O41	2.629	Ligand to solvent $H_2O\cdots H_2O$
O43···O19	2.499	Solvent to ligand $H_2O\cdots COOH$
O43···O17	2.791	Solvent to ligand $H_2O\cdots COOH$
O44···O9	2.579	Solvent to ligand $H_2O\cdots COOH$
O44···O7	2.872	Solvent to ligand $H_2O\cdots COOH$

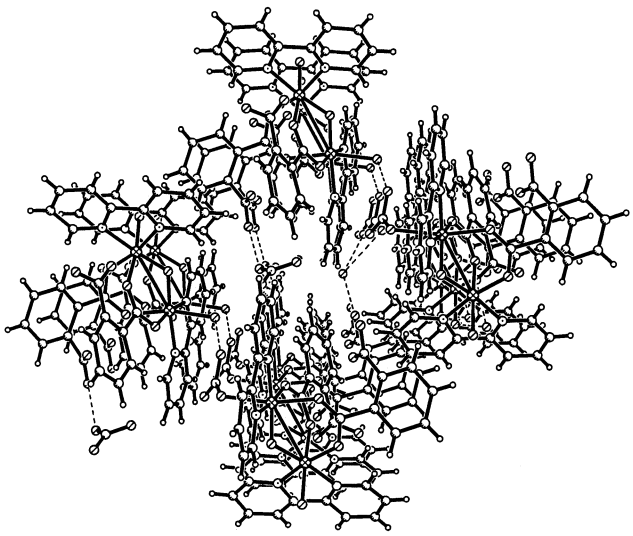

Fig. 4. Packing diagram of unit cell of $\mathbf{2}\cdot 5H_2O$, showing the network structure formed by hydrogen bonding interactions.

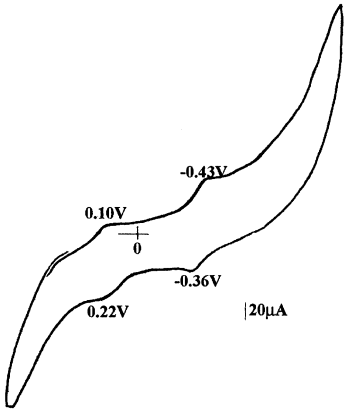

Fig. 5. Cyclic voltammogram of **2** (1 mM) in DMF with scan speed 200 mV s^{-1}. Peak potentials are indicated.

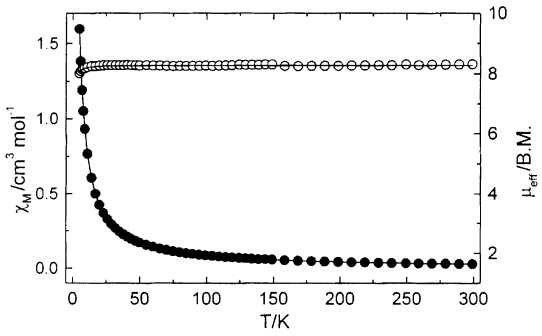

Fig. 6. Experimental molar susceptibility (χ_M) and effect magnetic moment (μ_{eff}) of temperature dependence for compound **1**. The solid line represents the calculated values.

of the effective magnetic moments (μ_{eff}) and molar susceptibilities (χ_M) in Fig. 6. At room temperature, μ_{eff} amounts to 8.32 BM, which is the value expected for two independent spins $S = 5/2$ (8.37 BM for $g = 2$). When the temperature decreases in the range 300–30 K, the μ_{eff} value remains quite constant (8.32–8.29 BM). At lower temperature ($T < 30$ K), a decrease in μ_{eff} was observed, which may arise from zero-field splitting of $S = 5/2$. To take this effect into account, the theoretical expression of magnetic susceptibility for the complex is as follows:

$$\chi_{\parallel} = \frac{Ng_z^2\beta^2}{4KT}\left[\frac{1 + 9\exp(-2D/KT) + 25\exp(-6D/KT)}{1 + \exp(-2D/KT) + \exp(-6D/KT)}\right] \quad (1)$$

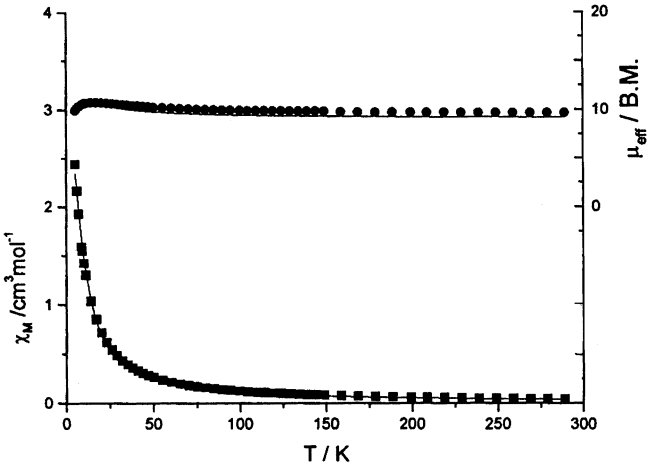

Fig. 7. Experimental molar susceptibility (χ_M) and effect magnetic moment (μ_{eff}) of temperature dependence for compound **2**. The solid line represents the calculated values.

and $F = 1.48 \times 10^{-5}$. This fitting result supports the occurrence of significant zero-field splitting in the Mn(II) ions.

The magnetic behavior of **2** is represented in Fig. 7 as the temperature dependence of μ_{eff} and χ_M, respectively. χ_M is the corrected molar magnetic susceptibility per $Mn_2\cdots Mn_2$ unit. At room temperature μ_{eff} is equal to 9.65 BM close to that expected for uncoupled four $S = 2$ spins (9.79 BM for $g_{Mn} = 2$). The effective magnetic moment smoothly increases with the decrease of the temperature, reaching a maximum value ($\mu_{eff} =$ 10.78 BM) around 14 K, and finally slightly decreases below 14 K. This behavior is quite characteristic of a ferromagnetic interaction between the neighboring Mn(III) ions. The structure of the complex consists of both virtually isolated and very similar binuclear Mn_2 units. The expected μ_{eff} value of 12.65 BM is not reached for two isolated $S = 4$ ground states, indicating zero-field splitting effect in the ground state for per binuclear Mn_2 unit. To take this effect into account, an expression of the magnetic susceptibility χ_{bi} of the binuclear Mn_2 unit was used from the spin Hamiltonian in zero field. This expression is based on the fact that only zero-field splitting for the ground state was considered [12] and that the Zeeman splitting was treated isotropically for the sake of simplicity [13]:

$$\chi_{\perp} = \frac{Ng_x^2\beta^2}{4}\left[\frac{(9/KT + 8/D) - 11\exp(-2D/KT)/2D - 5\exp(-6D/KT)/2D}{1 + \exp(-2D/KT) + \exp(-6D/KT)}\right] \quad (2)$$

$$\chi = \frac{2\chi_{\perp} + \chi_{\parallel}}{3} \quad (3)$$

where D is the axial zero-field splitting parameter for the Mn(II) ion and $g_x = g_z = g$. A least-squares fitting of the experimental data led to $D = 1.77$ cm^{-1}, $g = 1.98$

$$\hat{H} = -2J\hat{S}_1\cdot\hat{S}_2 - D[S_Z^2 - S(S+1)/3] \quad (4)$$

where D is the axial zero-field splitting parameter for the $S = 4$ state. Using Eq. (4), a susceptibility equation for the binuclear Mn_2 unit is given as follows:

$$\chi_{bi} = \frac{2Ng^2\beta^2}{KT}\left[\frac{A}{B}\right] \quad (5)$$

$$A = 16\exp\left(\frac{28D}{3KT}\right) + 9\exp\left(\frac{7D}{3KT}\right) + 4\exp\left(\frac{-8D}{3KT}\right) + \exp\left(\frac{-17D}{3KT}\right) + 14\exp\left(\frac{-8J}{KT}\right) + 5\exp\left(\frac{-14J}{KT}\right) + \exp\left(\frac{-18J}{KT}\right)$$

$$B = \exp\left(\frac{-20D}{3KT}\right) + 2\exp\left(\frac{28D}{3KT}\right) + 2\exp\left(\frac{7D}{3KT}\right) + 2\exp\left(\frac{-8D}{3KT}\right) + 2\exp\left(\frac{-17D}{3KT}\right) + 7\exp\left(\frac{-8J}{KT}\right) + 5\exp\left(\frac{-14J}{KT}\right) + 3\exp\left(\frac{-18J}{KT}\right) + \exp\left(\frac{-20J}{KT}\right)$$

For **2** containing tetranuclear manganese, which consists of two independent binuclear Mn_2 units, the magnetic susceptibility equation becomes

$$\chi_{tetra} = 2\chi_{bi} = \frac{4Ng\beta^2}{KT}\left[\frac{A}{B}\right] \quad (6)$$

The least-squares fitting of the experimental data led to $J = 2.37\ cm^{-1}$, $g = 2.02$ and $D = 0.75\ cm^{-1}$ with $R = 1.45 \times 10^{-3}$. As reported in literature [3a,b,4a,d] for a series of (μ-oxo)bis(μ-carboxylato)dimanganese-(III) complexes, the two Mn(III) ions undergo a weak magnetic exchange interaction in the range $-5 < J < 10\ cm^{-1}$. It should be pointed out that the values for D and J are overall values. In the case of the coexistence of two Mn_2 sites in compound **2**, the different Mn sites may cause the change of the J value. Refering to other dinuclear Mn(III) analogs, weak magnetic exchange occuring between the Mn(III) sites is expected for compound **2**. However, it is difficult to discuss precisely which structural features will result in the weak ferromagnetic exchange for compound **2**. A further study will be required.

Acknowledgements

This work was supported by State Key Basic Research and Development Plan of China (G1998010100) and NNSFC (Nos. 29733090, 29973047 and 39970177).

References

[1] (a) K. Wieghardt, Angew. Chem., Int. Ed. Engl. 28 (1989) 1153;
(b) G. Christou, Acc. Chem. Res. 22 (1989) 328;
(c) V.L. Pecoraro, M.J. Baldwin, A. Gelasco, Chem. Rev. 94 (1994) 807.

[2] P. Nordlund, B.M. Sjöberg, H. Eklund, Nature 345 (1990) 593.

[3] (a) J.B. Vincent, H.L. Tsai, A.G. Blackman, S. Wang, P.D.W. Boyd, K. Folting, J.C. Huffman, E.B. Lobkovsky, D.N. Hendrickson, G. Christou, J. Am. Chem. Soc. 115 (1993) 12353;
(b) M. Corbella, R. Costa, J. Ribas, P.H. Fries, J.-M. Latour, L. Öhrström, X. Solans, V. Rodríguez, Inorg. Chem. 35 (1996) 1857;
(c) K.R. Reddy, M.V. Rajasekharan, S. Sukumar, Polyhedron 23 (1996) 4161;
(d) S. Ménage, J.J. Girerd, A. Gleizes, J. Chem. Soc., Chem. Commun. (1988) 431;
(e) J.B. Vincent, K. Folting, J.C. Huffman, G. Christou, Biochem. Soc. Trans. 16 (1988) 822;
(f) A.G. Blackman, J.C. Huffman, E.B. Lobkovsky, G. Christou, J. Chem. Soc., Chem. Commun. (1991) 989.

[4] (a) K. Wieghardt, U. Bossek, D. Ventur, J. Weiss, J. Chem. Soc., Chem. Commun. (1985) 347;
(b) J.E. Sheats, R.S. Czernuszewicz, G.C. Dismukes, A.L. Rheingold, V. Petrouleas, J. Stubbe, W.H. Armstrong, R.H. Beer, S.J. Lippard, J. Am. Chem. Soc. 109 (1987) 1435;
(c) K. Wieghardt, U. Bossek, B. Nuber, J. Weiss, J. Bonvoisin, M. Corbella, S.E. Vitols, J.J. Girerd, J. Am. Chem. Soc. 110 (1988) 7398;
(d) F.J. Wu, D.M. Kurtz, K.S. Hagen, P.D. Nyman, P.G. Debrunner, V.A. Vankai, Inorg. Chem. 29 (1990) 5174;
(e) S. Mahapatra, T.K. Lal, R. Mukherjee, Inorg. Chem. 33 (1994) 1579;
(f) K. Wieghardt, U. Bossek, J. Bonvoisin, P. Beauvillain, J.J. Girerd, B. Nuber, J. Weiss, J. Heinze, Angew. Chem., Int. Ed. Engl. 25 (1986) 1030.

[5] (a) R.C. Squire, S.M.J. Aubin, K. Folting, W.E. Streib, G. Christou, D.N. Hendrickson, Inorg. Chem. 34 (1995) 6463;
(b) M.W. Wemple, H.L. Tsai, S. Wang, J.P. Clude, W.E. Streib, J.C. Huffman, D.N. Hendrickson, G. Christou, Inorg. Chem. 35 (1996) 6437;
(c) Z.-H. Jiang, S.-L. Ma, D.-Z. Liao, S.-P. Yan, G.-L. Wang, X.-K. Yao, R.-J. Wang, J. Chem. Soc., Chem. Commun. (1993) 745.

[6] MolEN, An Interactive Structure Solution Procedure, Enraf–Nonius, Delft, The Netherlands, 1990.

[7] G.M. Sheldrick, SHELXTL-93, Program for the Refinement of Crystal Structure, University of Göttingen, Germany.

[8] (a) X.-M. Chen, X.-Y. Huang, Y.-J. Xu, Y.-J. Zhu, J. Chem. Crystallogr. 25 (1995) 605;
(b) X.-M. Chen, R.-Q. Wang, Z.-T. Xu, Acta Crystallogr., Sect. C 51 (1995) 820;
(c) X.-M. Chen, K.-L. Shi, Acta Crystallogr., Sect. C 51 (1995) 358;
(d) P.O. Lumme, E. Lindell, Acta Crystallogr., Sect. C 44 (1988) 463;
(e) X.-L. Yu, Y.-X. Tong, X.-M. Chen, T.C.W. Mak, J. Chem. Crystallogr. 27 (1997) 441.

[9] C. Philouze, M. Henry, N. Auger, D. Vignier, M. Lance, M. Nierlich, J.-J. Girerd, Inorg. Chem. 38 (1999) 4.

[10] E. Libby, K. Folting, C.J. Huffman, J.C. Huffman, G. Christou, Inorg. Chem. 32 (1993) 2549.

[11] (a) N. Arulasmy, J. Glerup, A. Hazell, D.J. Hodgson, C.J. McKenzie, H. Toftlund, Inorg. Chem. 33 (1994) 3023;
(b) K.J. Oberhausen, R.J. O'Brien, J.F. Richardson, R.M. Buchanan, R. Costa, J.M. Latour, H.L. Tsai, D.N. Hendrickson, Inorg. Chem. 32 (1993) 4561.

[12] Y. Journanx, O. Kahn, J. Zarembowitch, J. Galy, J. Jaud, J. Am. Chem. Soc. 105 (1983) 7585.

[13] G. Aromi, M.J. Knapp, J.P. Claude, J.C. Huffman, D.N. Hendrickson, G. Christou, J. Am. Chem. Soc. 121 (1999) 5489.